Sigma Journal of Engineering and Natural Sciences
Web page info: https://sigma.yildiz.edu.tr
DOI: 10.14744/sigma.2024.00007

Research Article

Eriocitrin derivatives and their anthelmintic potentials

Dilara KARAMAN[1,*], Ahmet Onur GİRİŞGİN[2], Oya GİRİŞGİN[3]

[1]Department of Bioengineering, Yildiz Technical University, İstanbul, 34220, Türkiye
[2]Department of Parasitology, Veterinary Faculty, Bursa Uludag University, Bursa, 16059, Türkiye
[3]Karacabey Vocational School, Bursa Uludag University, Bursa, 16700, Türkiye

ARTICLE INFO

Article history
Received: 03 October 2022
Revised: 24 March 2023
Accepted: 12 April 2023

Keywords:
Anthelmintic; CPT 2; Docking; Eriocitrin Derivatives; Molecular Modelling

ABSTRACT

De novo drug design focused on *in silico* research of more effective and safe drugs is the essential stage of pharmacophore-based drug discovery. This study aimed to evaluate the anthelmintic potential of herbal ligand derivatives to suggest new drug scaffolds and examine fragment-based key-lock fit models of drug candidates to offer more potent drugs. The reversible inhibitors of the Carnitine Palmitoyltransferase 2 enzyme (CPT 2) have been evaluated as anthelmintic drug candidates because the increased CPT 2 substrate in the environment leads to the death of the nematode. Eriocitrin is a herbal molecule found in several plants, especially in the citrus peel. It has never been previously investigated for anthelmintic purposes, but it is a molecule found in some anthelmintic plants. Therefore, eriocitrin was determined as the scaffold of a novel anthelmintic drug candidate. To design new eriocitrin derivatives, positions 3 and 8 on the chromene ring of eriocitrin were chosen to insert five different side groups, such as hydrogen, propylsulfanyl, acetate, phenol, and aniline. Twenty-four derivatives designed with Biovia Discovery Studio 2020 Client were docked with the antinematodal drug target rat CPT 2 using AutoDock4.2 software. ADME properties and the binding mode of the most potent derivative were investigated. For the derivative with the best-scored molecule E05, the free binding energy was -9.08 kcal/mol, and the K_i value was calculated as 22.017 nM. E05, which had a better inhibition value than eriocitrin showed that the presence of phenol at the 3rd position in the chromene nucleus of eriocitrin facilitated CPT 2 inhibition. This research is the first study that shows the eriocitrin and E05 are potent anthelmintic molecules according to *in silico* docking tests. E05 is worth to be investigated comprehensively with further *in vitro* studies.

Cite this article as: Karaman D, Girişgin AO, Girişgin O. Eriocitrin derivatives and their anthelmintic potentials. Sigma J Eng Nat Sci 2024;42(3):875–884.

INTRODUCTION

Helminths are among the critical factors that affect productivity in animals and cause disease and low productivity, especially in ruminants. Gastrointestinal (GI) nematodes generally have a chronic course and the most significant economic impact is due to subclinical infections that cause

*Corresponding author.
*E-mail address: dilara.karaman@std.yildiz.edu.tr

This paper was recommended for publication in revised form by Editor in-Chief Ahmet Selim Dalkılıç

reduced growth, milk yield and fertility [1]. On the other hand, lungworm infections can create an immediate economic burden on the farm due to deaths and sharp declines in milk yield [2]. The anthelmintic drugs to be developed should have a broad therapeutic index, be easily administered, and be economical and effective in a single dose to protect the animal's health. Since infections with nematodes living in the gastrointestinal tract of mammals are often chronic, designing new drug candidates using computational tools is an essential task for researchers. Carnitine Palmitoyltransferase 2 (CPT 2) (EC 2.3.1.21) in the transferase class is an enzyme located in the inner membrane of mitochondria, an asymmetric monomer protein with a length of 626 amino acids consisting of A and B chains. It is essential in the beta-oxidation of long-chain fatty acids [3]. The CPT 2 enzyme, used in the experiments in silico as an antinematodal drug target, is one of the enzymes defined as a "metabolic checkpoint" in nematodes. It was shown by Tyagi et al. (2018) that the inhibition of CPT 2 affects the vital functions of the nematode and leads to the death of some nematode species, such as Onchocerca linealis [4]. Although CPT 2 enzyme has a vital role in mammals, reversible CPT 2 inhibitors are potentially useful tools for removing of destructive nematodes. While the short-term inhibition of the CPT 2 enzyme in the host animal does not harm the host, the increased CPT 2 substrate in the environment leads to the death of the nematode. The importance of using the crystalline structure of the rat CPT 2 enzyme in docking experiments for the development of new antinematodal drugs was demonstrated by Taylor et al. (2013) [5] and Tyagi et al. (2018) [4]. Knowing the centre coordinates of a binding cavity for CPT 2 enzyme crystalline structure is a cause to prefer the CPT 2 in silico anthelmintic research. Hence CPT 2 enzyme is an available target to examine the antinematodal property of a reversible drug candidate. Eriocitrin is an eriodictyol derivative mostly found in lemon peel, and it is formed by adding O-β-rutinoside at the 7th position to eriodictyol. This chromene derivative flavonoid has anti-inflammatory and antioxidant properties [6, 7]. Eriocitrin has been isolated from the citrus peel and the leaves of mint (*Mentha piperita*) and is one of the flavonoid glycosides responsible for the antiallergic action of *M. piperita* [8]. *M. piperita* extract has also been shown to inhibit helminth egg development [9].

Eriocitrin also has an antiproliferative effect [10]. However, it has not been investigated yet whether it had an ovicidal impact that could be related to the antiproliferative effect. While protein-ligand docking simulations performed with in silico molecular modelling method constitute the first step of drug development studies, they provide researchers with initial data on target-drug interactions at the atomic level. Such computational experiments have great importance for reducing the workload in drug development. To develop new drugs, the relevant drug scaffolds need to be discovered. For this, herbal products that have not been tried before but have the possibility of effect are tested on the target organism. However, these in vivo experiments involve long-term studies and have a severe cost. Therefore, investigating the inhibition properties of drug candidate components through computer-aided drug design (CADD) significantly reduces the time and cost required for drug research [11]. Although the antidepressant [12], antidiabetic [13], and antitumor [14] properties of eriocitrin have been investigated in previous studies, its anthelmintic properties have never been studied. The anthelmintic effect of the citrus (*Citrus limon* L.) peel, which is rich in eriocitrin, was demonstrated by Upadhyaya (2018) on earthworms of the *Eicinia foetida* species [15]. *Origanum vulgare* type thyme, which has eriocitrin in its infusion, is a plant with anthelmintic effects. Castro et al. (2013) revealed that it had ovicidal effects on the eggs of *Haemonchus contortus* type helminths found in farm animals [16]. Hence, it is a need to research the anthelmintic property of eriocitrin on target organisms or target proteins. Specifically, *in silico* molecular modelling studies with eriocitrin should be increased because the absorption of the eriocitrin in the gastrointestinal system is low, and the period of staying in the blood is concise. Therefore, *in silico* experiments should be a priority and loaded in the eriocitrin investigations.

In the current study, twenty-four novel eriocitrin-based derivatives were designed to investigate whether they could be more potent than eriocitrin in anthelmintic terms. These derivatives were compared in terms of free binding energies and K_i values due to docking simulation with AutoDock4.2. The derivative with the best score was examined in terms of its location and chemical interactions in CPT 2, and the most potent eriocitrin derivative was passed through the criteria of the SwissADME web server to evaluate whether it could be a drug candidate. The interaction network of eriocitrin in CPT 2 was compared with the derivative possessing the best score. These comparisons provided the first data to understand the structure-activity relationship in developing a new eriocitrin-based anthelmintic. It is the first study to demonstrate the anthelmintic property of eriocitrin and its derivatives via in silico molecular dockings. The possible chemical interactions of eriocitrin with CPT 2 enzyme were shown and interpreted for the first time.

MATERIAL AND METHODS

Experimental Procedure

While the placements of derivative molecules in the CPT 2 enzyme were examined according to the key-lock fit model, docking simulation was performed with AutoDock4.2 [17] and ADT (AutoDock Tools) [18, 19] programs. Possible chemical interactions of ligands in the binding region of the protein were investigated with Biovia Discovery Studio 2020 Client [20]. The Linux operating

system was used to perform the docking simulation on the Intel core processor Asus laptop computer.

Preparation of Proteins

Biovia Discovery Studio 2020 Client program was used for protein preparation. For this purpose, the crystal structure of Rattus norvegicus Carnitine palmitoyltransferase 2 (CPT 2) enzyme (PDB code: 2H4T, resolution: 1.90 Å, bound with dodecane (C12H26)) [3] was obtained from Brookhaven Protein Databank (http://www.rcsb.org/pdb) in May 2020. The CPT 2 enzyme of R. norvegicus was obtained by expression from *Escherichia coli* by Hsiao et al., and its 3D structure was demonstrated by the X-ray diffraction method in 2006. All water molecules, non-interacting ions and inhibitors in this protein, whose macromolecular structure is a monomer consisting of A and B chains, have been deleted from the pdb file. All hydrogen atoms have been added. "Clean Geometry" tool and Charmforcefield were used to optimise the protein. The procedure used by Yelekçi et al. (2013) was partially guided in the preparation of the protein [21].

Preparation of Ligands

To design a de novo anthelmintic drug, eriocitrin was used as the scaffold in this study. Eriocitrin is found in the citrus peel (*Citrus sinensis* L.) and Istanbul thyme (*Origanum vulgare* subsp. *hirtum*), which have anthelmintic effects. However, the anthelmintic effect of eriocitrin has never been researched before. Eriocitrin was taken from the Pubchem [22] database and converted to pdb format with the OpenBabel [23] program. Positions 3 and 8 of the chromene ring were chosen to insert the R groups (Figure 1). Substituted R groups are hydrogen (-H), acetate (CH3COO-), phenol (-C6H6O), aniline (-C6H5NH2) and propylsulfanyl (C3H7S-).

Two criteria were taken into consideration in the selection of subgroups; 1) being a side group found in the existing drug structure or the structure of anthelmintic herbal molecules, 2) being an aromatic side group that will be able to synthesized and will increase possible chemical interactions.

Accordingly, the propylsulfanyl group was chosen as a side group because it is in the structure of Albendazole, a highly preferred drug in the benzimidazoles group, and allicin, a highly effective anthelmintic herbal ligand in the content of garlic (*Allium sativum* L.), has a sulphur component.

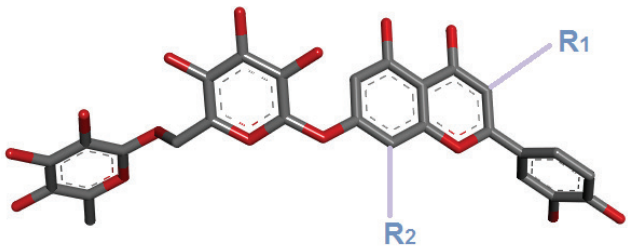

Figure 1. Substitution of R groups on eriocitrin chosen as the scaffold.

Acetate was chosen as another side group because it can allow the formation of hydrogen bonds with the oxygen atoms in its structure. Phenol and aniline were selected because they are two groups that can increase aromatic interactions and be easy to synthesize. Hydrogen was chosen to understand the effect when no side group is added (in other words, the effect of the other added group alone). The 3rd and 8th positions were chosen because the chromene ring is very similar to the coumarin ring, and the 3rd and 8th positions are used to design synthesizable bioactive coumarin derivatives. Derivative molecules were drawn with Discovery Studio 2020 Client (Biovia Inc.) and optimized with "Clean Geometry", a fast Drieden-like minimization tool. Derivative molecules in pdb format were converted to pdbqt format with ADT [18, 19] program.

Molecular Docking

Coordinates given by Taylor et al. (2013) were used for the docking simulation of the CPT 2 enzyme, and the x, y, z coordinates accepted as the center were: 61.752, 72.800 and 52.032 [5]. In the docking procedure, the protein was kept rigid, but the hydrogen atoms were allowed to be released only in their movement at the active site of the protein. The dielectric constant was set to 10, ionic strength 0.145, grid box dimensions 60×60×60 and grid point 0.375 Å. Since the number of rotational bonds is less than 10, the maximum generation number is set to 27 000, and the maximum development number is 2 500 000. The Lamarckian genetic algorithm was used. The Autodock4.2 program was selected for the entire docking procedure. A docking simulation was performed with 20 runs.

Prediction of Adme

According to the results of the docking simulations of the derivative molecules, the ADME (Absorption, Distribution, Metabolism, Excretion) properties of the eriocitrin derivative molecule with the highest binding affinity were estimated via the SwissADME [24] web server. The SwissADME web tool provides free access to a repository of fast yet robust predictive models for physicochemical properties, pharmacokinetics, similarity and availability for medicinal chemistry, including competent in-house methods such as BOILED-Egg, iLOGP and Bioavailability Radar. The Bioavailability Radar is monitored for rapid assessment of drug similarity. Lipophilicity, molecular size, polarity, solubility, flexibility and saturation properties are taken into account in the creation of this radar graph [24]. The six properties in the Bioavailability Radar are among the most basic criteria chosen to show whether the physicochemical and pharmacokinetic values expected from a bioavailable component are within reasonable limits. According to the Bioavailability Radar, the molecular weight

(MA) for a bioavailable component should be between 150-200 g/mol, TPSA should be between 20-130 Å^2, lipophilicity (XLOGP3) should be between -0.7 and +5.0, the carbon fraction in sp3 hybridization, which is a saturation indicator, should not be less than 0.25, and solubility (log S) should not be more than 6 [24], water solubility score should be between 1-3 (1, highest solubility, 5, lowest solubility), the number of rotatable bonds should be between 0-9 [25].

An estimation based on computational methods was made by comparing their ability to penetrate the blood-brain barrier, gastrointestinal absorption, and oral bioavailability via the SwissADME web server (Table 2).

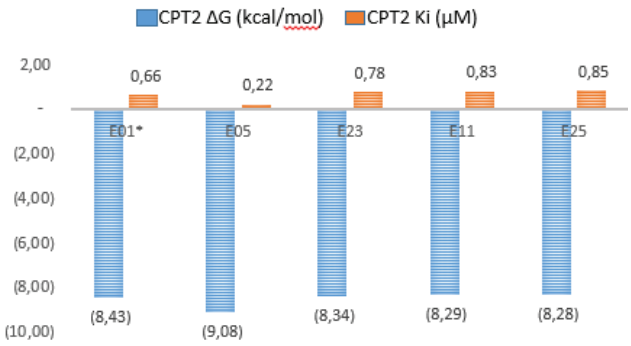

Figure 2. K_i and ΔG values for CPT 2 inhibition of the first four ligands and eriocitrin (E01) had the best score values as a result of docking.

RESULTS AND DISCUSSION

Among these derivatives, the K_i values of the first 4 molecules with the best result in terms of inhibition constant (K_i) are shown in Table 1 and Figure 2. According to the graph, these molecules are E05, E23, E11 and E25. The groups these derivatives carry in their 3rd and 8th positions are respectively as follows; E05: phenol and hydrogen, E11: hydrogen and propylsulfanyl, E23: propylsulfanyl and phenol, E25: phenol and phenol.

Figure 3A shows possible localizations of 5 ligands (four derivatives and eriocitrin) within CPT2. In a volume of approximately 24×24×24 Å^3, it is seen that the molecules mostly overlap, while the flexibility due to the rotational bonds of the ligands causes the different conformations shown in the figure. Different groups at positions 3 and 8 also play an important role in the changes seen in the placement of the molecule within the active site of the protein (Figures 3A and 3B).

In the four derivatives in Figure 3B, located so close to each other that they can be called almost congruous, the most differentially located derivative is E25, indicated by turquoise. E25 carries phenol in the 3rd and 8th positions. Among the ligands whose K_i values are given in Figure 2, the derivative with the best value is E05. The interactions of E05 with CPT 2 are shown in detail in Figure 4. Conventional hydrogen bonding was formed between the oxygen atom of the GLY375 residue and the H70 atom of the ligand at a distance of 1.86 Å (shown in green), and a repulsion force was estimated between the same oxygen and the H71 atom of the ligand at a distance of 1.6 Å (indicated in red) (Figure 4A). A conventional hydrogen bond occurred at a distance of 1.45 Å between SER488 and the hydrogen in the 3-hydroxy group of the dihydroxy phenyl ring in the 2nd position in the chromene ring of the ligand (Figure 4B).

In Figure 5A, it is seen that eriocitrin forms hydrogen bonds with six different residues in their interactions within the CPT 2 enzyme. These residues are TRP 116, ASP 376, SER 590, TYR 486, ASN 130 and TYR 120. However, an undesirable donor-donor repulsion force was predicted at a distance of 2.63 Å between ASN 585 and the two hydroxyl groups on the glycoside structure of eriocitrin (Figure 5B).

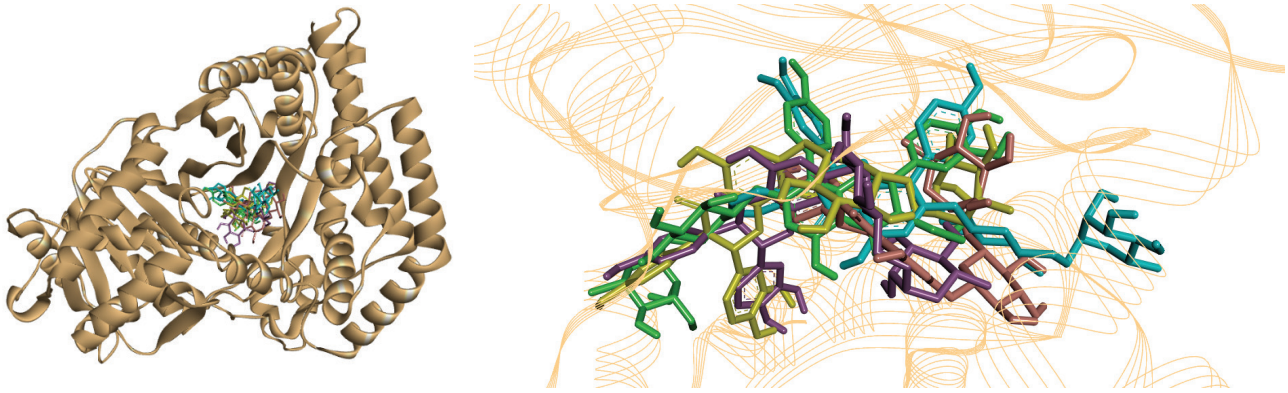

(a) (b)

Figure 3. Localizations of four derivative molecules possessing the best binding affinity a) E05, E11, E23, E25 and eriocitrin (E01) in CPT 2. E01 is pink, E05 is purple, E11 is yellow, E23 is green, and E25 is turquoise, protein is an orange solid ribbon. b) Near perspective to ligands at the binding site. CPT 2 is shown in a 3D structure with orange lines.

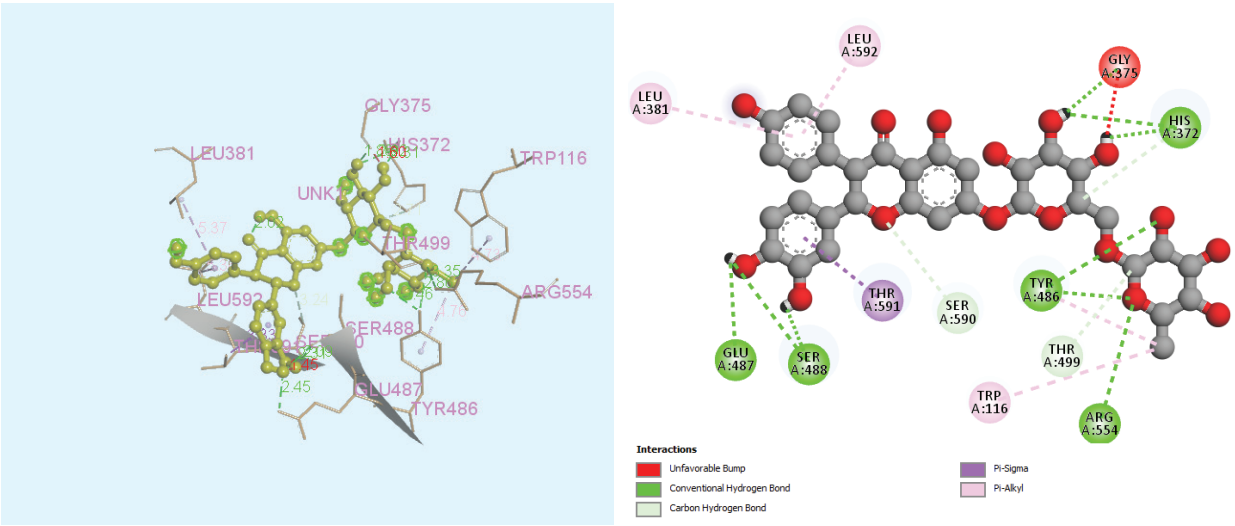

(a) (b)

Figure 4. Chemical interactions of E05, which has the best score among 24 derivatives, in CPT 2. a) E05 in 3D representation in the yellow ball and stick structure, surrounding residues in thin stick structure, interactions in dashed lines, b) In 2D representation, red and green dashed lines represent conventional hydrogen bonds, purple π-sigma bonds, pink π-alkyl bonds.

This condition may have prevented to fall the binding energy a little more. The fact that the E05 is not subject to such a repulsion force has allowed it to show a better score value. In the 3D representation in Figure 5A, eriocitrin is shown in the center with the ball and stick model and the residues with which it interacts are shown with the thin stick model. In the 2D representation in Figure 5B, residues with which it interacts are represented by colored spheres.

As shown in Figure 3A and comparing Figure 4B and Figure 5B, E05 is positioned in the opposite direction of the eriocitrin and this difference has brought a significant energy difference. An interesting conformation in Figure 5A is that the rutinoside group of the eriocitrin stands at a right angle compared to the rutinoside group of E05. The rotation in the bond where the rutinoside attaches to the chromene ring has led to this conformation and thus

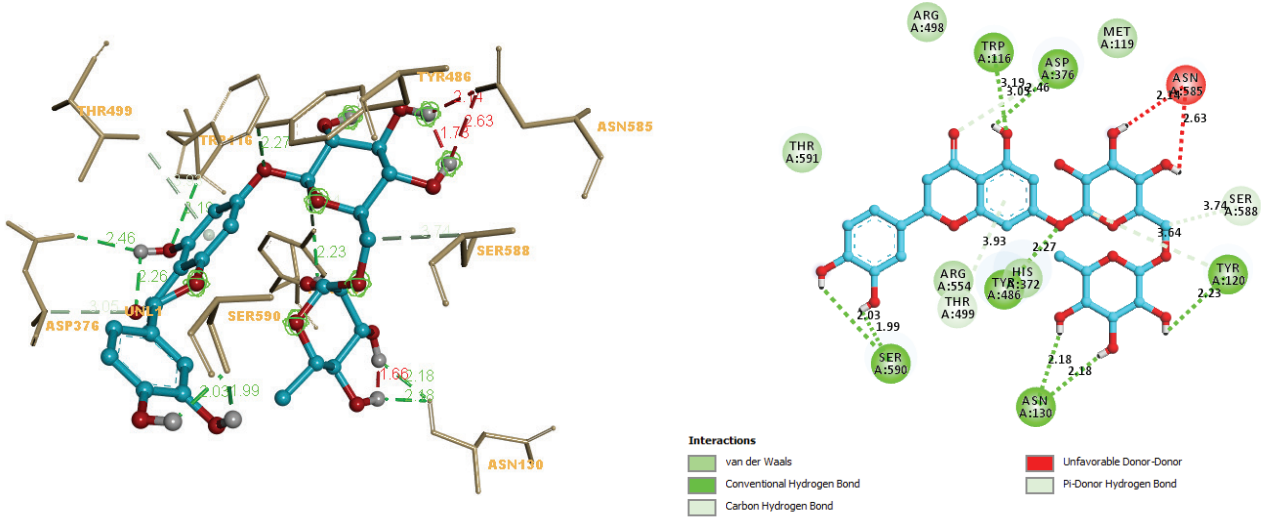

(a) (b)

Figure 5. Chemical interactions of eriocitrin (E01) in CPT 2. a) In the 3D representation, eriocitrin is shown in the center with the ball and stick model and the residues with which it interacts are shown with the thin stick model. b) In 2D representation, residues with which it interacts are represented by colored spheres.

different interactions. While the dihydroxyphenyl group of eriocitrin enters between the α-helix and the beta-sheet structure shown in Figures 3A and 3B, the phenol group located at the 3rd position of E05 seems to approach another looping structure. The two residues with which E05 interacts on this loop structure appear to be LEU 381 and LEU 592 and make pi-alkyl interactions with these amino acids (see Figures 4A and 4B).

Free binding energies and K_i values of 24 derivative molecules calculated using AutoDock4.2 are given in Table 1. The values in the table show that twelve (50%) of the derivatives had ΔG values greater than -7 kcal/mol. Among these derivatives, the derivative with the lowest binding affinity with CPT 2 is E12. This derivative molecule substituted acetate at position 3 and propylsulfanyl at position 8, which reduces affinity. The docking results of the derivatives in the table generally show K_i values at the micromolar level. The difference between the free binding energies of the derivatives with the best and worst results is -3.8 kcal/mol.

Table 2 shows the important properties of the ligand possessing the lowest binding energy, such as oral bioavailability, gastrointestinal (GI) absorption, and penetrating the blood-brain barrier, according to the SwissADME web server. Since the molecular weight (MW) of the drawn derivative molecule, E05 is greater than 500, the number of OH (hydroxyl groups) in the molecule is more than 5, and the number of oxygen atoms is more than 10, it does not comply with three of Lipinski's rules. It also does not provide the rules of Muegge, Veber and Ghoose. Since E05 has MW>600, TPSA>150, the number of H acceptors>10 and the number of H donors>5, it does not even comply with the rules of the most tolerant Muegge. This derivative molecule cannot penetrate the blood-brain barrier and has poor GI absorption. However, with these properties, it is advantageous for the removal of nematodes in the GI. Because if E05 stays in the GI longer and higher concentration, nematodes will be affected more. The region shown with red convex in the bioavailability radar graph in Table 2 shows that the molecular polarity of E05 is at the highest level and its size is quite large, while the flexibility, lipophilicity, unsaturation and insolubility values remain within reasonable limits. From a pharmacokinetic point of view, it is desirable that the TPSA value of the drug be less than 140 Å^2. The lipophilicity value of E05 was calculated as Log P (XLOGP3) 0.88 and the TPSA (topological polar surface area) as 265.5 Å^2.

Table 1. Docking results of derivative molecules

Derivative molecule	R1	R2	CPT 2 ΔG (kcal/mol)	CPT 2 K_i (μM)
E01 (Eriocitrin)	H	H	-8.43	0.66349
E02	CH3COO-	H	-6.83	9.85
E03	C3H7S-	H	-7.29	4.55
E04	-C6H5NH2	H	-7.66	2.41
E05	-C6H6O	H	-9.08	0.22017
E06	H	CH3COO-	-6.28	24.75
E07	CH3COO-	CH3COO-	-5.98	41.11
E08	C3H7S-	CH3COO-	-5.96	42.90
E09	-C6H5NH2	CH3COO-	-7.61	2.62
E10	-C6H6O	CH3COO-	-6.18	29.69
E11	H	C3H7S-	-8.29	0.83333
E12	CH3COO-	C3H7S-	-5.28	133.88
E13	C3H7S-	C3H7S-	-6.73	11.61
E14	-C6H5NH2	C3H7S-	-6.82	10.00
E15	-C6H6O	C3H7S-	-8.01	1.33
E16	H	-C6H5NH2	-8.04	1.28
E17	CH3COO-	-C6H5NH2	-6.06	36.03
E18	C3H7S-	-C6H5NH2	-6.01	39.31
E19	-C6H5NH2	-C6H5NH2	-7.78	1.97
E20	-C6H6O	-C6H5NH2	-7.50	3.16
E21	H	-C6H6O	-6.36	21.73
E22	CH3COO-	-C6H6O	-7.57	2.85
E23	C3H7S-	-C6H6O	-8.34	0.77585
E24	-C6H5NH2	-C6H6O	-6.88	9.10
E25	-C6H6O	-C6H6O	-8.28	0.85338

Table 2. ADME related features of E05 (calculated with SwissADME web server)

Conformation of E05	Bioavailability radar of E05
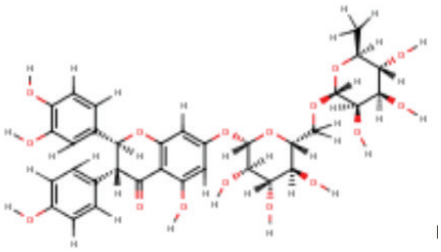	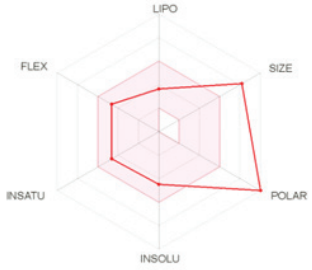

Physicochemical Properties	
Formula	C33H36O16
Molecular weight	688.63 g/mol
Num. rotatable bonds	7
Num. H-bond acceptors	16
Num. H-bond donors	10
Num. heavy atoms	49
Num. arom. heavy atoms	18
Fraction Csp3	0.42
Molar Refractivity	163.45
TPSA	265.52 $Å^2$
Water Solubility	
Log S (ESOL)	-4.47
Solubility	2.31e-02 mg/ml; 3.36e-05 mol/l
Class	Moderately soluble
Log S (Ali)	-6.04
Solubility	6.28e-04 mg/ml; 9.11e-07 mol/l
Class	Poorly soluble
Log S (SILICOS-IT)	-1.48
Solubility	2.29e+1 mg/ml; 3.32e-02 mol/l
Class	Soluble
Lipophilicity	
Log $P_{o/w}$ (iLOGP)	1.71
Log $P_{o/w}$ (XLOGP3)	0.88
Log $P_{o/w}$ (WLOGP)	-0.68
Log $P_{o/w}$ (MLOGP)	-2.78
Log $P_{o/w}$ (SILICOS-IT)	-1.45
Consensus Log $P_{o/w}$	-0.46
Pharmacokinetics	
GI absorption	Low
BBB permeant	No
P-gp substrate	Yes
Log K_p (skin permeation)	-9.88 cm/s
CYP1A2, CYP2C19, CYP2C9, CYP2D6, CYP3A4 inhibitor	No
Druglikeness	
Lipinski	No, 3 violations; MW>500, NorO>10, NHorOH>5
Ghose, Veber, Egan, and Muegge	No
Bioavailability Score	0.17

GI: Gastrointestinal, BBB: Blood-brain barrier, P-gp: P-glycoprotein, Fraction Csp3: carbon ratio in sp3 hybridization, TPSA: Topological Polar Surface Area, MW: Molecular Weight, FLEX: Flexibility, LIPO: Lipophilicity, SIZE: Size, POLAR: Polarity, INSOLU: Insolubility, INSATU: Insaturation

CPT 2 is localized to the inner membrane of mitochondria [26]. It has a role in the conversion of acetyl-coenzyme A (CoA) to fatty acyl-CoA while providing β-oxidation of fatty acids [27]. Limited number of CPT 2 inhibitors have been discovered recently. Some of these inhibitors are called Etomoxir, ST1326 (Teglicar), Perhexiline, and Oxfenicine [28]. Taylor et al. (2013) docked the rat CPT-2 enzyme (PDB ID: 2H4T) and its inhibitor Perhexiline by using the Autodock4 program. The major residues in contact with Perhexiline were P133, F134, M135, F370, H372, D376, G377, V378, L381, S590, G601, and F602. They showed that H372 was the catalytic residue. A hydrogen bond has formed between the amine group of Perhexiline and the carbonyl group of D376. As for in our study L381, H372, G375, Y486, G487, S488, T499, R554, S590, T591, and L592 were the residues that interacted with E05, and W116, M119, Y120, N130, H372, D376, Y486, R498, T499, N585, S588, and T591 interacted with eriocitrin in the CPT 2 enzyme binding site. Also, a hydrogen bond was seen between D376 and eriocitrin. H372 interacted with both E05 and eriocitrin which supports the insight of catalytic residue. The residues that differ between mammals and nematodes in the amino acid sequence of the CPT 2 enzyme are L335, S445, Q447, V597, S598, L599, A615, W620, C623, and N624 [5]. According to the results of our study, both eriocitrin and its derivative E05 did not interact with any of these different residues. Hence eriocitrin or E05 can bind both CPT 2 enzymes in nematodes and mammals.

An experimental study conducted in Italy showed that different extracts of *O. vulgare* inhibited the hatching of gastrointestinal nematodes in cattle by a percentage ranging from 8.8% to 100%. Dry and hydroalcoholic extracts were the most promising inhibitors, according to the study. Given this ovicidal property, *O. vulgare* may be an important source of antiparasitic compounds for nematodiosis control in ruminants. The mean per cent inhibition upon hatching *O. vulgare* hydroalcoholic extract at a concentration of 80 mg/mL was 96.7% [16]. Although the anthelmintic effect of *O. vulgare* was shown and eriocitrin is a component of it, it has never been investigated whether its anthelmintic effect was due to eriocitrin. The in silico data in the present study is a candidate to show this relation.

Mentha piperita extract inhibited the hatching of *Haemonchus contortus* eggs by approximately 90% at a concentration of 0.078 mg/mL [9]. It was shown by Inoue et al. (2012) that *M. piperita* leaves contain eriocitrin [8]. Eriocitrin is one of the five flavonoids detected in the 50% ethanolic extract of orange peel, and this extract showed a high antiproliferative effect [10]. For this reason, the antiproliferative effects of eriocitrin derivatives and, accordingly, their ovicidal effects should be investigated in vitro. As for in our study, the first data on the anthelmintic effects of eriocitrin and its derivatives were presented. The possible molecular mechanisms of the antioxidant and antiproliferative effects of these molecules and the anthelmintic results which will be created by these effects should be revealed by further research. In order to increase the inhibition of CPT2, other derivatives should be designed and tested on the basis of aglycans that do not carry a routinosid group and thus may have higher gastrointestinal absorption, and more potent components should be discovered.

According to the literature, the component showing the strongest antiradical activity in orange peel (*Citrus sinensis* L.) is eriocitrin. The fact that the two hydroxyl groups attached to the B ring are in the ortho position and related to each other plays a role in this activity of eriocitrin. Because the antiradical activity of hesperidin, which is formed as a result of the replacement of one of these groups with the methoxy group, was found to be weaker than eriocitrin [29].

Two of the main flavonoids found in the methanolic extract of the leaves of *Mentha pulegium* L collected from the Bizerte region of Tunisia are eriocitrin and luteolin. Eriocitrin is the most abundant flavonoid (20.1-25.3 mg/g in dry matter). The methanolic extract showed significant antimicrobial activities as well as high antioxidant and radical scavenging activity [30]. Its potential to get stronger the host's immune system due to its antioxidant potency and antiradical activities makes eriocitrin a more valuable point in the research for anthelmintic purposes because a strong immune system is capable of suppressing the proliferation and spread of parasites.

CONCLUSION

According to the results of in silico docking simulations obtained in our study, E05 is a candidate to show a better antinematodal activity than eriocitrin among some eriocitrin-based derivative molecules. Extra groups added to the chromene ring change the affinity. The addition of phenol to the 3rd position allows for better binding energy to CPT 2. Half of the derivatives designed on the basis of eriocitrin in this study were found to have a free binding energy of less than -7 kcal/mol. E05, which is predicted to be more potent than eriocitrin among the designed derivatives, may be useful in the development of a new antinematodal drug. These findings comprise the first data on the anthelmintic potential of eriocitrin and its derivatives. Drug designers and pharmacologists can evaluate these results to research in vitro activities of potential anthelmintic herbal ligands and their derivatives. Since *Onchocerca linealis* is a target of CPT 2 inhibitors, this result shows that eriocitrin or E05 can be tried for removing *O. linealis* in vitro studies. Because of the relation of *O. linealis* with *Onchocerca volvulus*, these studies can also open a new perspective to evaluate the removal of *O. volvulus* causing River blindness. In fact, every year thousands of people are blind due to *O. volvulus*, however, the only drug is Ivermectin which can treat River blindness. The drug resistance problem against Ivermectin is a potential danger for endemic regions. Hence eriocitrin and its derivatives may be new drug candidates,

and they should be investigated more in order to develop new anthelmintics for *O. volvulus* treatment.

ACKNOWLEDGEMENTS

We would like to dedicate this article to our esteemed Professor, the deceased Prof. Dr. Metin Aktaş. We are grateful to him for supporting science and scientists always. No financial support was received from any institution in the making of this study. The authors declared that there is no conflict of interest.

AUTHORSHIP CONTRIBUTIONS

Authors equally contributed to this work.

DATA AVAILABILITY STATEMENT

The authors confirm that the data that supports the findings of this study are available within the article. Raw data that support the finding of this study are available from the corresponding author, upon reasonable request.

CONFLICT OF INTEREST

The author declared no potential conflicts of interest with respect to the research, authorship, and/or publication of this article.

ETHICS

There are no ethical issues with the publication of this manuscript

REFERENCES

[1] Morgan E, Charlier J, Hendrickx G, Biggeri A, Catalan D, von Samson-Himmelstjerna G, et al. Global change and helminth infections in grazing ruminants in Europe: Impacts, trends and sustainable solutions. Agriculture 2013;3:484–502. [CrossRef]

[2] Holzhauer M, van Schaik G, Saatkamp HW, Ploeger HW. Lungworm outbreaks in adult dairy cows: Estimating economic losses and lessons to be learned. Vet Rec 2011;169:494. [CrossRef]

[3] Hsiao YS, Jogl G, Esser V, Tong L. Crystal structure of rat carnitine palmitoyltransferase II (CPT-II). Biochem Biophys Res Commun 2006;346:974–80. [CrossRef]

[4] Tyagi R, Maddirala AR, Elfawal M, Fischer C, Bulman CA, Rosa BA, et al. Small molecule inhibitors of metabolic enzymes repurposed as a new class of anthelmintics. ACS Infect Dis 2018;4:1130–1145. [CrossRef]

[5] Taylor CM, Wang Q, Rosa BA, Huang SC, Powell K, Schedl T, et al. Discovery of anthelmintic drug targets and drugs using chokepoints in nematode metabolic pathways. PLoS Pathog 2013;9:e1003505. [CrossRef]

[6] Guo G, Shi W, Shi F, Gong W, Li F, Zhou G, et al. Anti-inflammatory effects of eriocitrin against the dextran sulfate sodium-induced experimental colitis in murine model. J Biochem Mol Toxicol 2019;33:e22400. [CrossRef]

[7] Miyake Y, Yamamoto K, Osawa T. Isolation of eriocitrin (eriodictyol 7-rutinoside) from lemon fruit (Citrus limon BURM. f.) and its antioxidative activity. Food Sci Technol Int 1997;3:84–89. [CrossRef]

[8] Inoue T, Sugimoto Y, Masuda H, Kamei C. Antiallergic effect of flavonoid glycosides obtained from Mentha piperita L. Biol Pharm Bull 2002;25:256–259. [CrossRef]

[9] Carvalho CO, Chagas AC, Cotinguiba F, Furlan M, Brito LG, Chaves FC, et al. The anthelmintic effect of plant extracts on Haemonchus contortus and Strongyloides venezuelensis. Vet Parasitol 2012;183:260–268. [CrossRef]

[10] Diab KA, Shafik RE, Yasuda S. In Vitro Antioxidant and Antiproliferative Activities of novel orange peel extract and it's fractions on Leukemia HL-60 cells. Asian Pac J Cancer Prev 2015;16:7053–7060. [CrossRef]

[11] Eren D, Yalçın İ. The aim of implementation of the molecular mechanic and the molecular dynamic methods in rational drug design. J Fac Pharm Ankara 2020;44:334–355. [Turkish]

[12] Uivarosi V, Munteanu AC, Nițulescu GM. An Overview of Synthetic and Semisynthetic Flavonoid Derivatives and Analogues: Perspectives in Drug Discovery. In: Rahman AU, editor. Studies in natural products chemistry. Amsterdam: Elsevier; 2019. p. 29–84. [CrossRef]

[13] Li N, Wang LJ, Jiang B, Li XQ, Guo CL, Guo SJ, et al. Recent progress of the development of dipeptidyl peptidase-4 inhibitors for the treatment of type 2 diabetes mellitus. Eur J Med Chem 2018;151:145–157. [CrossRef]

[14] Niaz K, Khan F. Analysis of Polyphenolics. In: Silva AS, Nabavi SF, Saeedi M, Nabavi SM. Recent advances in natural products analysis. Amsterdam: Elsevier; 2020. p. 39–197. [CrossRef]

[15] Upadhyaya S. Citrus limon L Burmf peel: Potential anthelmintic agent against Indian Earthworm Eicinia foetida. J Drug Deliv Ther 2018;8:248–250. [CrossRef]

[16] Castro LLDD, Madrid IM, Aguiar CLG, Castro LMD, Cleff MB, Berne MEA, et al. Origanum vulgare (Lamiaceae) ovicidal potential on gastrointestinal nematodes of cattle. Ciênc Anim Bras 2013;14:508–513.

[17] Morris GM, Goodsell DS, Halliday RS, Huey R, Hart WE, Belew RK, et al. Automated docking using a Lamarckian genetic algorithm and an empirical binding free energy function. J Comput Chem 1998;19:1639–1662. [CrossRef]

[18] Huey R, Morris GM, Olson AJ, Goodsell DS. A semiempirical free energy force field with charge-based desolvation. J Comput Chem 2007;28:1145–1152. [CrossRef]

[19] Morris GM, Huey R, Lindstrom W, Sanner MF, Belew RK, Goodsell DS, et al. AutoDock4 and AutoDockTools4: Automated docking with selective receptor flexibility. J Comput Chem 2009;30:2785–2791. [CrossRef]

[20] BIOVIA Dassault Systèmes. Discovery Studio Modeling Environment. Release 2020, San Diego: Dassault Systèmes; 2020.

[21] Yelekçi K, Büyüktürk B, Kayrak N. In silico identification of novel and selective monoamine oxidase B inhibitors. J Neural Transm (Vienna) 2013;120:853–858. [CrossRef]

[22] Kim S, Chen J, Cheng T, Gindulyte A, He J, He S, et al. PubChem in 2021: New data content and improved web interfaces. Nucleic Acids Res 2021;49:D1388–D1395. [CrossRef]

[23] O'Boyle NM, Banck M, James CA, Morley C, Vandermeersch T, Hutchison GR. Open Babel: An open chemical toolbox. J Cheminform 2011;3:33. [CrossRef]

[24] Daina A, Michielin O, Zoete V. SwissADME: A free web tool to evaluate pharmacokinetics, drug-likeness and medicinal chemistry friendliness of small molecules. Sci Rep 2017;7:42717. [CrossRef]

[25] Ritchie TJ, Ertl P, Lewis R. The graphical representation of ADME-related molecule properties for medicinal chemists. Drug Discov Today 2011;16:65–72. [CrossRef]

[26] Bonnefont JP, Djouadi F, Prip-Buus C, Gobin S, Munnich A, Bastin J. Carnitine palmitoyltransferases 1 and 2: Biochemical, molecular and medical aspects. Mol Aspects Med 2004;25:495–520. [CrossRef]

[27] McGarry JD, Brown NF. The mitochondrial carnitine palmitoyltransferase system. From concept to molecular analysis. Eur J Biochem 1997;244:1–14. [CrossRef]

[28] Wang J, Xiang H, Lu Y, Wu T, Ji G. The role and therapeutic implication of CPTs in fatty acid oxidation and cancers progression. Am J Cancer Res 2021;11:2477–2494.

[29] Sroka Z, Fecka I, Cisowski W. Antiradical and anti-H2O2 properties of polyphenolic compounds from an aqueous peppermint extract. Z Naturforsch C J Biosci 2005;60:826–832. [CrossRef]

[30] Jebali J, Ghazghazi H, Aouadhi C, ELBini-Dhouib I, Ben Salem R, Srairi-Abid N, et al. Tunisian Native Mentha pulegium L. Extracts: Phytochemical composition and biological activities. Molecules 2022;27:314. [CrossRef]